DROUGHT HAZARD ASSESSMENT USING ANOMALY DROUGHT INDEX AND GEOGRAPHIC INFORMATION SYSTEM IN THE CHI RIVER BASIN, THAILAND

***Sarunphas IAMAMPAI*[1], *Jirawat KANASUT*[1], *Banramee KANTAWONG*[1] *and Prem RANGSIWANICHPONG*[1*]**

DOI: 10.21163/GT_2023.181.04

ABSTRACT:
Drought is a natural disaster that causes problems in agriculture. Such events have been frequented in the Chi River basin, Thailand, in the last 10 years. Currently, drought assessment is conducted in several ways, including the use of product data from satellites or meteorological and hydrological data. In this study, we developed the anomaly drought index (ANDI) based on a combination of normalized difference vegetation index and soil water index product data and runoff station data using the entropy weight method. The ANDI was created and compared to historical data from the Emergency Events Database (EM-DAT) and drought-related data from 2011 to 2020. The ANDI shows a correlation with 0.80 with rice yield and 0.9 with reservoir (dry), and 0.95 with rainfall (wet). Furthermore, we classified ANDI's drought intensity into three categories: mild, moderate, and severe. Droughts were discovered to have occurred in 2013, 2015, 2016, 2019, and 2020. They began in wet seasons and materialized in the subsequent dry seasons. These results were consistent with the drought reports of EM-DAT and the National Hydroinformatics Data Center. Therefore, the ANDI is suitable for assessing drought in the Chi River basin in Thailand.

Key-words: *Natural hazard, NDVI, Remote Sensing, Spatial analysis, Thailand.*

1. INTRODUCTION

Drought is the one of natural disasters that occurs in several countries, and its impact can huge damage to environmental, energy, and human activities, especially agriculture (Wilhite et al., 2007). Generally, drought hazard occurred by a prolonged lack of precipitation or insufficient rainfall (Kallis, 2008; Dracup et al., 1980). Additionally, extended periods of precipitation deficit deplete surface water and groundwater reservoirs (Marcos-Garcia et al., 2017). Thailand frequently experiences droughts and is one of the most drought-affected countries in Southeast Asia (Pandey et al., 2007). Its agricultural sector is directly affected by droughts. Most of the Thai people are farmers and are often affected by drought. The damage from droughts in Thailand is concentrated in the northeastern part of the country, given the large area used for rice cultivation in this region (Prabnakorn et al., 2018). In 2004‑2005 and 2015‑2017, drought events in Thailand occurred with high damage to economic system approximately $220 million and $330 million, respectively (Wichitarapongsakun et al., 2016).

Several researchers have developed drought indices for analyzing drought hazards using meteorological and satellite data (Anderson et al., 2016; Cui et al., 2021). Drought indices are mostly analyzed based on precipitation data; they include the Palmer drought severity index (Palmer, 1965), standard precipitation index (SPI) (McKee et al., 1993), and standard precipitation evapotranspiration index (SPEI) (Vicente-Serrano et al., 2010). Despite all of these indices, the SPI is the most suitable for assessing drought in rain-fed areas, but not for irrigated areas (Teweldebirhan et al., 2019). The normalized difference vegetation index (NDVI) can represent quantified vegetation based on satellite data and connected to drought occurrences. It is calculated from red and infrared reflectances.

[1]*Department of Water Resources Engineering, Faculty of Engineering, Kasetsart University, Bangkok 10900, Thailand, sarunphass@gmail.com, jirawat.g@ku.th, kobe.baramee@gmail.com. corr. author*[*]*prem.r@ku.th*

The NDVI is widely used to indicate vegetation health because it can detect chlorophyll well (Tucker, 1979; Amri et al., 2011; Rouse et al., 1974). The soil water index (SWI) is a drought index developed from a fusion of surface soil moisture (SSM) observations from the Sentinel-1 C-band SAR and Metop ASCAT sensors; it is calculated via recursive formulation. The SWI has eight characteristic T values for various soil depths (Bauer-Marschallinger et al., 2018; Albergel et al., 2008; Brocca et al., 2010). The global drought index (GDI) was developed based on a combination of the NDVI and SWI. The GDI varies between areas with different land uses (Zribi et al., 2021). The composite drought indicator is a drought index calculated by a weighted combination of the SPI, NDVI, evapotranspiration, and land surface temperature (Bijaber et al., 2018). These studies show that composite drought indices can better identify drought hazard areas than single indices.

In this study, we developed a new index (Anomaly Drought Index [ANDI]) using the Entropy Weight (EW) method for analyzing the drought hazard in the Chi River basin by combining runoff station data, SPI, NDVI, and SWI. In addition, drought reports from relevant agencies were used for comparison to verify the accuracy of the drought assessment results obtained from the ANDI.

2. STUDY AREA

The Chi River basin is a major watershed in northeast Thailand. It has an area of 49,131 km^2 (**Fig. 1**) and consists of the following provinces: Chaiyaphum, Khon Kaen, Nong Bua Lamphu, Udon Thani, Maha Sarakham, Nakhon Ratchasima, Loei, Phetchabun, Kalasin, Roi Et, Yasothon, Ubon Ratchathani, Sisaket, and Mukdahan.

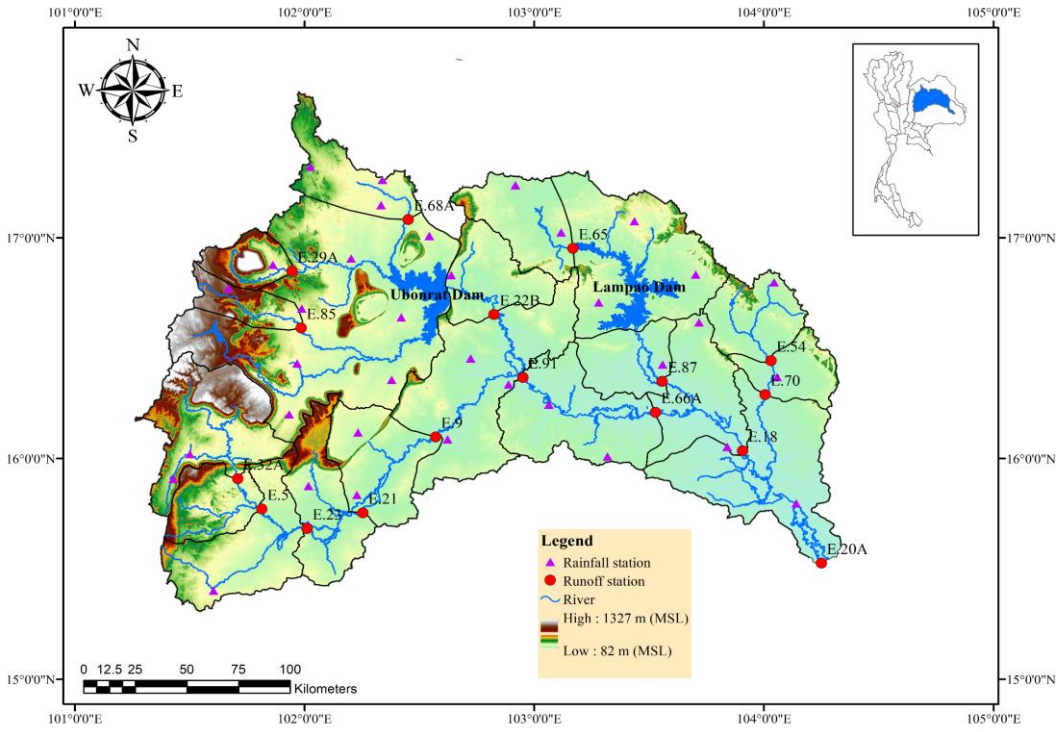

Fig. 1. Topography map of the Chi River basin.

The climate in the Chi River basin is influenced by northeast and southeast monsoons, which result in a dry season (November‑April) and a wet season (May‑October), respectively. Annual rainfall in the Chi River basin averages approximately 1,285 mm and more than 90% of rainfall occurs in the wet season (**Table 1**).

Table 1.

Monthly average rainfall in the Chi River basin.

month	1	2	3	4	5	6	7	8	9	10	11	12	sum
average rainfall (mm)	12	7	36	56	150	136	242	309	253	67	16	1	1285

There are two large, important reservoirs, namely, the Ubon Rat Reservoir and the Lampao Reservoir, which have storage capacities of 2,431 million and 1,980 million m^3, respectively. According to land use data produced by the Department of Land Development in 2016, agricultural land accounts for 70% of the total area, whereas forest land accounts for 19% (**Fig. 2**). In the dry season, normally farmers planted rice crop during December-January. For harvesting activities is usually between March and April.

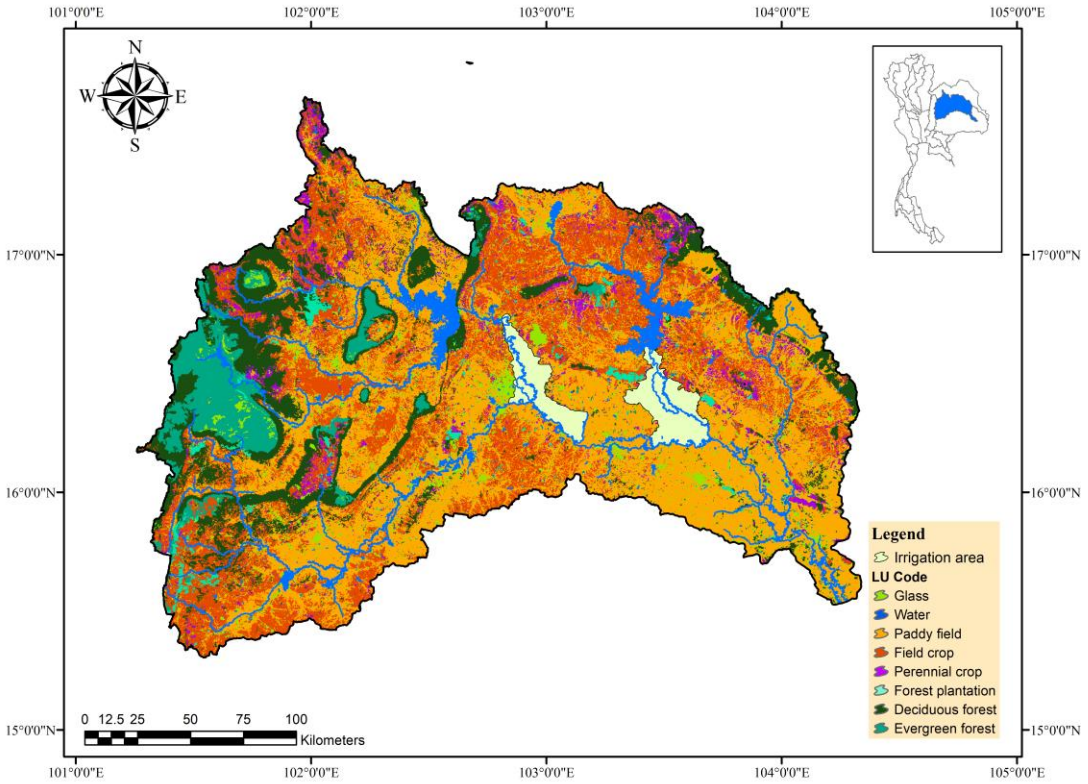

Fig. 2. Land used map of the Chi River basin.

3. DATA AND METHODS

In this study, we used data from 15 runoff stations operated by the Royal Irrigation Department (RID), observed monthly runoff data from 2011 to 2020 (10 years), data from two large reservoirs (Ubon Rat and Lampao dam), and rice yield during dry season data (collected by the RID). The monthly rainfall data were collected by 37 rain gauge stations of the Thai Meteorological Department during 2010 to 2020 for calculating SPI. Furthermore, we gathered land use data from the Land Development Department. We then generated a drought hazard map for the Chi River basin using remote sensing data and a geographic information system (GIS).

In 1993, the SPI was developed by Mckee et al., which it based only on monthly precipitation data. The SPI can be described using Eqs. (1)-(3) (Asadi Zarch, M.A. et al. 2014).

$$H(x_k) = q + (1-q)G(x_k) \tag{1}$$

For $0 < H(x_k) < 0.5$

$$SPI = -\left(t - \frac{c_0+c_1t+c_2t^2}{1+d_1t+d_2t^2+d_3t^3}\right),\ t = \sqrt{ln\left(\frac{1}{H(x_k)^2}\right)} \tag{2}$$

For $0.5 < H(x_k) < 1.0$

$$SPI = \left(t - \frac{c_0+c_1t+c_2t^2}{1+d_1t+d_2t^2+d_3t^3}\right),\ t = \sqrt{ln\left(\frac{1}{(1-H(x_k))^2}\right)} \tag{3}$$

the $G(x_k)$ is Gamma probability density function, q is the probability of zero precipitation and $H(x_k)$ is the cumulative probability. Where c_0 = 2.515517, c_1 = 0.802853, c_2 = 0.010328, d_1 = 1.432788, d_2 = 0.189269, and d_3 = 0.001308.

The SWI, which was included to represent the water content, is a product of the Copernicus Global Land Service (https://land.copernicus.eu/global/products/swi accessed on 1 March 2022). The SWI has a daily spatial resolution of 10 km^2 and a characteristic temporal length (T) parameter that includes 1, 5, 10, 15, 20, 40, 60, and 100 to reflect soil depth. (Albergel et al., 2008; Paulik et al., 2014). This index is highly correlated with soil moisture content, especially when the T length is 20 (Zribi et al., 2010). The SWI is calculated as Eqs. (4)-(6).

$$SWI(t_n) = \sum_i^n SSM(t_i)\, e^{-\frac{t_n-t_i}{T}} \Big/ \sum_i^n e^{-\frac{t_n-t_i}{T}} \tag{4}$$

$$SWI(t_n) = SWI(t_{n-1}) + K_n(SSM(t_n) - SWI(t_{n-1})) \tag{5}$$

$$K_n = K_{n-1}/(K_{n-1} + e^{-(\frac{t_n-t_{n-1}}{T})}) \tag{6}$$

the variables t_n and t_{n-1} are the current and previous dates, respectively, in Julian days. T is the parameter of characteristic time length. *SSM* is Surface Soil Moisture observations from Sentinel-1 C-band SAR and Metop ASCAT sensors. K_n is factor at time n. The initial value of SWI_0 and K_0 were set = 1.

The NDVI, an effective remote sensing indicator of green vegetation distribution, is derived by determining the difference in spectral reflectance value between the red and NIR bands (Rouse Jr et al., 1974). Additionally, the NDVI can indicate the growing conditions of plants (Bharathkumar et al., 2015; Gillespie et al., 2018) and is used for drought monitoring (Son et al., 2012; Nanzad et al., 2019). Generally, the NDVI value ranges between −1 and 1 and can be calculated as in Eq. (7). In this study, we used NDVI values from MODIS (MOD13A2). The MOD13A2 product is corrected for atmospheric conditions, has a resolution of 1 km^2, and is provided every 16 days (https://e4ftl01.cr.usgs.gov/MOLT/MOD13A2.006 (accessed on 1 March 2022).

$$NDVI = \frac{NIR-RED}{NIR+RED} \tag{7}$$

where *NIR* denotes the near-infrared band and *RED* is the red band. They have wavelengths of 859 and 649 nm, respectively.

3.1. Relationship of drought indices

This method calculates data values in a way that indicates the change in such values for the same month in each year. Thus, the obtained data are not affected by the season. The standard anomaly time series is calculated by Eq. (8). Previously, the usual anomaly approach was utilized to determine the NDVI and SWI (Amri et al., 2011; Amri et al., 2012). To analyze drought without the influence of seasonality, we produced standard anomalies for the NDVI, SWI, and runoff data; we renamed the indices by adding Sa before the original names, thus, Sa-NDVI, Sa-SWI, and Sa-R. Due of its significant relationship to drought episodes in the Chi River basin, a 3-month cumulative runoff was used in drought estimate for Sa-R. The results shown that accumulated runoff from the previous 3 months (Sa-R) is strongly related to the drought events in the Chi River basin.

The SPI was created to track precipitation shortages over time. These time scales describe the impacts of drought on various water supplies, which have two timings for detecting drought: 1. short durations (1-6 months) and 2. long timescales (12-36 months). In this study, the SPI's 6-month cumulative rainfall was estimated.

$$Sa_i(\mathrm{x}) = \frac{X_i - X_{avg,i}}{\sigma_i} \tag{8}$$

where *X* denotes *SPI, SWI, NDVI*, and *Sa-R*. X_i is the data estimate for a given month *i*. $X_{avg,i}$ is the mean value of the data for month *i* generated from ten years of data. and σ_i is the standard deviation of the data during month *i* over the same 10-year period.

Additionally, we analyzed the relationship between the four indices (SPI, Sa-NDVI, Sa-SWI, and Sa-R) and the drought data (rice yield, rainfall, and water storage) by dividing the data into two seasonal groups (dry and wet seasons). Rice yield and water storage data were compared between dry season, and rainfall data was compared between wet season. The Pearson correlation coefficient is usually used to test relationships as Eq. (9).

$$R_{xy} = \frac{\sum_{i=1}^{n}(x_i - \bar{x})(y_i - \bar{y})}{\sqrt{\sum_{i=1}^{n}(x_i - \bar{x})^2 \sum_{i=1}^{n}(x_i - \bar{x})^2}} \tag{9}$$

where *x* is the indices (*SPI, Sa-SWI, Sa-NDVI, and Sa-R*) and *y* is the drought data (yield, rainfall, and water storage).

3.2. ANDI

In this research, we developed the ANDI for assessing the drought hazard in the Chi River basin. This new index was developed as a combination of SPI, Sa-SWI, Sa-NDVI, and Sa-R obtained from the same period, and it was computed by Eq. (10). The Entropy Weight (EW) was used to evaluate the criterion weight based on the intensity of the available data, and it calculated the weights of the four indices (*a*, *b*, *c*, and *d*) (Shannon et al., 1948). A specified variable will vary more the higher the entropy. The composite drought index weight is often determined using this approach (Chen et al., 2020, Waseem et al., 2015). The EW is computed as in Eqs. (11)-(14).

$$ANDI = a(SPI) + b(Sa\text{-}NDVI) + c(Sa\text{-}SWI) + d(Sa\text{-}R) \tag{10}$$

$$P_{ij} = \frac{x_{ij}}{\sum_{i=1}^{n} x_{ij}} \tag{11}$$

$$E_j = -\frac{1}{ln(n)}\sum_{i=1}^{n} P_{ijt}\, ln(P_{ij}) \tag{12}$$

$$D_j = 1 - E_j \tag{13}$$

$$Ew_j = \frac{D_j}{\sum_{j=1}^{n} D_j} \tag{14}$$

where i is i^{th} year (i = 1, 2, ... 10); X_{ij} is value of j index at the i^{th} year (j = 1, 2, 3, and 4 refer to *SPI*, *Sa-SWI*, *Sa-NDVI*, and *Sa-R*) and P_{ij} is the projection value that corresponds to the normalized value. E_j is entropy for j index; D_j is Degree of divergence for j index; Ew_j are the weights allocated to the variables.

The ANDI map, which was created using the SPI, Sa-NDVI, Sa-SWI, and Sa-R data sets, should aid in the efficiency of drought assessment in each sub-basin area. Because the NDVI and SWI data are held at spatial resolutions of 1 and 10 km^2, respectively, we aggregated the NDVI resolution to 10 km^2 by average value, which has the same resolution as SWI, and then computed it to the grid map of Sa-NDVI and Sa-SWI at 10 km^2 resolution. The SPI map was constructed by distributing rainfall station data to all grids with a resolution of 10 km^2 using the inverse distance squared technique (IDW), where rainfall station weights change with distance, as indicated in Eq (15). Then it was grid-calculated into the SPI grid map. We computed Sa-R from runoff station data at sub-basin outlets and used it to represent all grids in these sub-basins. The Sa-R grid map utilized in this study has 15 sub-basins with no reservoir area (See **Fig. 3** for the Sa-R map). Following that, the grid maps of Sa-NDVI, Sa-SWI, Sa-R, and SPI were weighted using the EW technique, which was derived using the grid as shown in **Fig.3.**

$$W_i = \frac{\frac{1}{d_i^2}}{\sum_{i=1}^{n}\left(\frac{1}{d_i^2}\right)} \tag{15}$$

where d_i is the distance between the runoff station and the considered grid location. W_i is the grid weighting of each rainfall station.

For effective drought assessment by ANDI. We determined three levels of severity for drought (mild, moderate, and severe) by comparing the ANDI values in the basin with quantities of rice yield and drought events recorded from EM-DAT. Drought conditions were represented by rice crops since the amount of rice cultivated between December and April of each year is determined by the amount of available water. However, droughts have the greatest impact on rice harvests.

3.3. Validation of ANDI via comparison of drought events recorded

The results of the ANDI drought map assessment in the Chi River basin were compared with the above drought levels. We divided the drought assessments into two seasons (dry and wet) and compared them with actual drought situations to analyze the relationship between them. We used drought reports for the Chi River basin from two sources, namely, the Centre for Research on the Epidemiology of Disasters (CRED) and the National Hydroinformatics Data Center (NHC). The CRED provides free access to the full Emergency Events Database (EM-DAT) for noncommercial purposes. EM-DAT is a global database containing details on the occurrences and effects of over 22,000 natural disasters, such as the number of people killed, injured, or affected and economic damage estimates. The NHC is maintaining a database for the management of water resources and natural disasters in Thailand. The NHC has been collecting records on water events for droughts and floods since 2005. **Fig. 4** shows a flowchart of the methodology in this study.

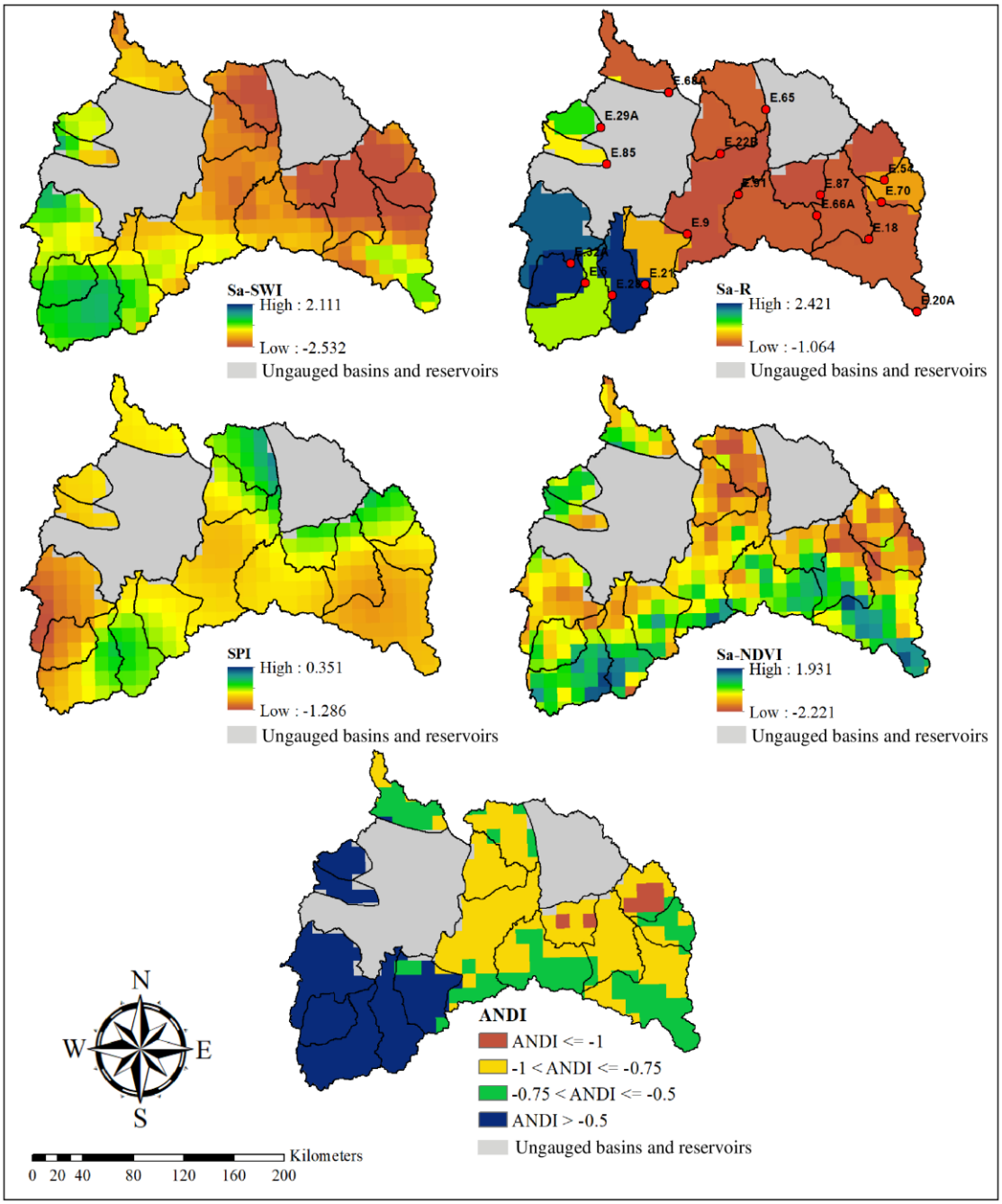

Fig. 3. Process of generating the ANDI map for assessing drought hazard (February 2013).

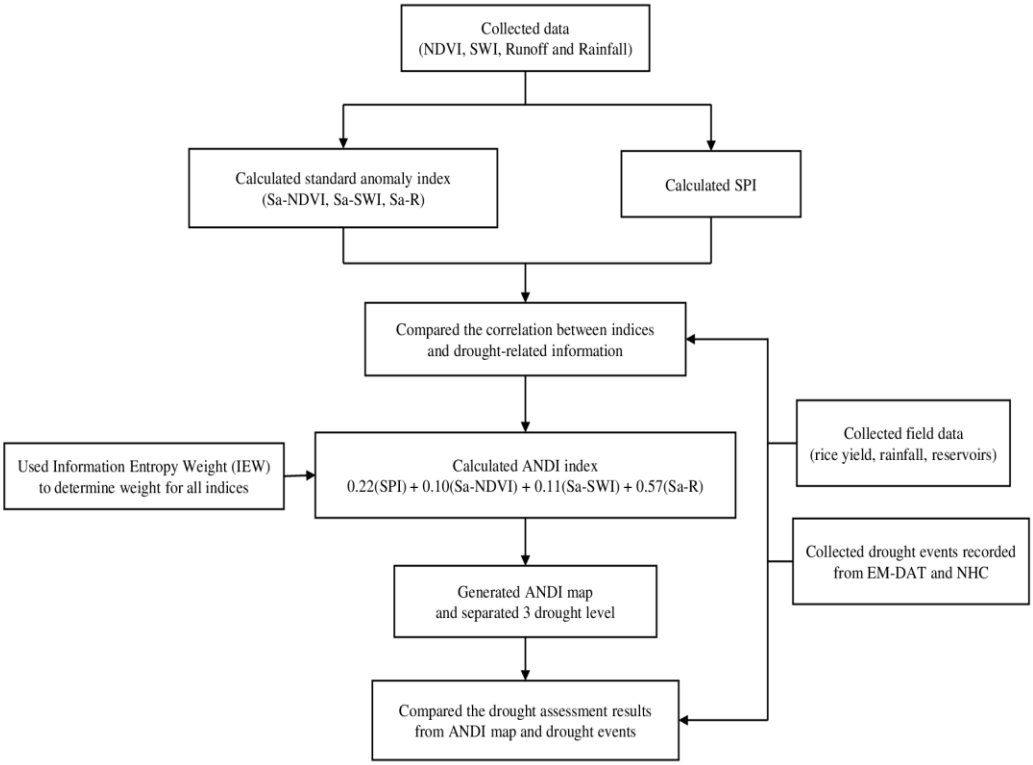

Fig. 4. Flowchart of the study methodology hazard.

4. RESULTS AND DISCUSSIONS

4.1. Relationship between drought indices and historical data

In the drought analysis for this study, **Fig. 5** shows the time series of the four data sets had distinct characteristics (SPI NDVI, SWI, and Runoff). The SPI demonstrates the change in cumulative rainfall at 6 months, and a negative value indicates that cumulative rainfall at 6 months is less than average. The remaining three data sets indicate that NDVI, SWI, and runoff are greater in the rainy season and lower in the dry season, with seasonality. Furthermore, each drought index reacts differently to drought occurrences. The NDVI is a useful tool for detecting changes in agricultural areas. However, it may not be suitable for non-agricultural locations. In December–April, the NDVI values in the irrigation area are clearly higher than those in the rain-fed area (**Fig. 6a**). This is because rice crops are cultivated in the irrigation area but not in the rain-fed area. **Fig. 6b** shows that the SWI values in the irrigated and rain-fed areas are nearly identical. Although the SWI accurately measures soil moisture content, the soil moisture that causes dryness in each place may differ, depending on the type of land use in that area. Additionally, the runoff data considered in this study directly shows the amount of water available to everyone, which accurately reflects the available quantity. However, it drops to zero during the dry season, making it difficult to quantify the severity of each year's drought (**Fig. 5d**).

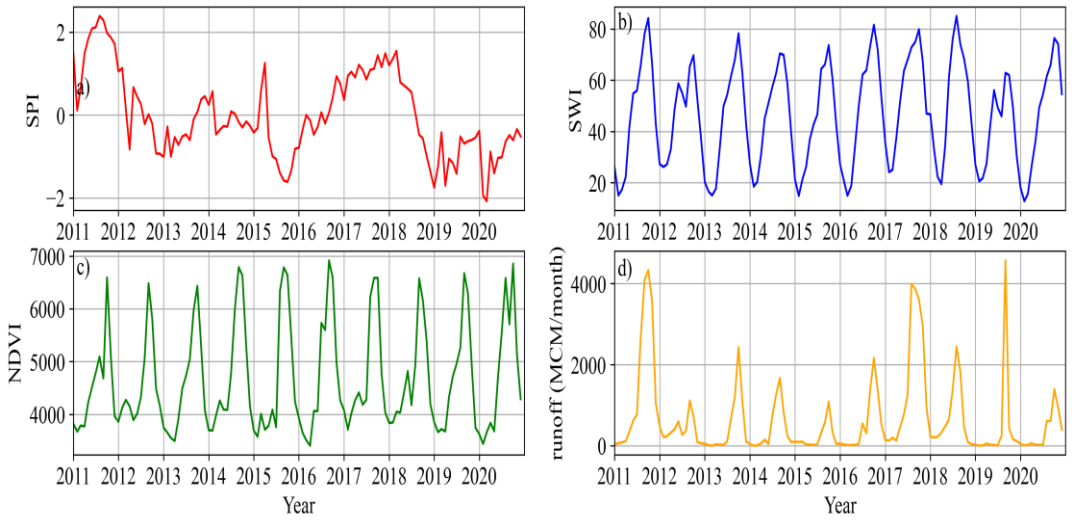

Fig. 5. SPI, NDVI, SWI, and monthly runoff (million cubic meters (MCM)/month) data time series from 2011–2020.

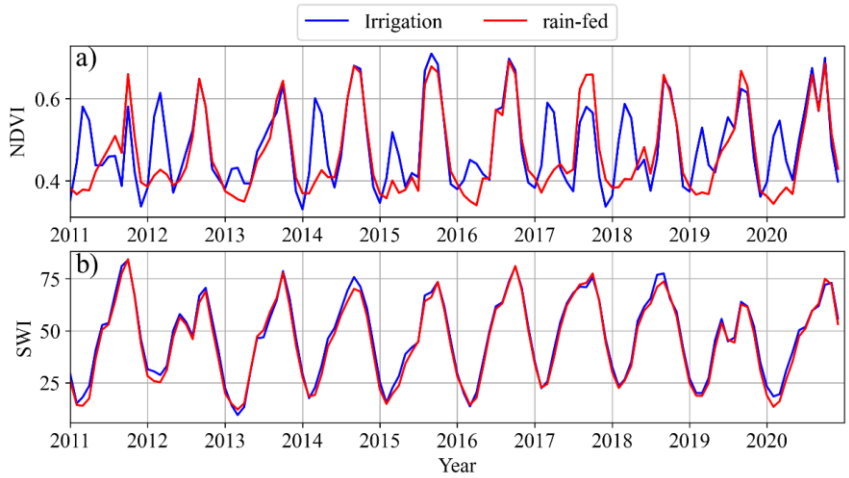

Fig. 6. SWI and NDVI time series in irrigation and rain-fed areas.

The results of the standard anomaly method (Sa-NDVI, Sa-SWI and Sa-R) are shown in **Fig. 7**, which can be separated into two main groups, namely, negative (the index is below the annual average for that month) and positive (the index is above the annual average for that month). These results indicate that if the standard anomaly value is negative during the dry season, then there is less soil moisture than typical. However, if it occurs during the rainy season, then rainfall is delayed or less than typical. The analysis of the seasonal correlation between the four indices and the measurement data (rice yield, reservoirs, and rainfall) reveals that, in dry seasons, Sa-R has the highest correlation with rice yields (0.86), followed by Sa-NDVI (0.67), SPI (0.61), and Sa-SWI (0.48), whereas SPI has the strong correlation with reservoir (0.88), followed by Sa-R (0.85), Sa-NDVI (0.77), and Sa-SWI (0.65). For the wet season, SPI is the most correlated with rainfall (0.96) and is followed by Sa-R (0.89), Sa-SWI (0.72), and Sa-NDVI (0.28) (**Table 2-3**). In addition, Sa-R stands out in its relationship to rice yield, while its relationship with reservoirs and rainfall is slightly less SPI. Although the Sa-R is more powerful than the others, it is a station data. When used as a representative of the sub-basin, it cannot see the difference between each pixel in sub-basins.

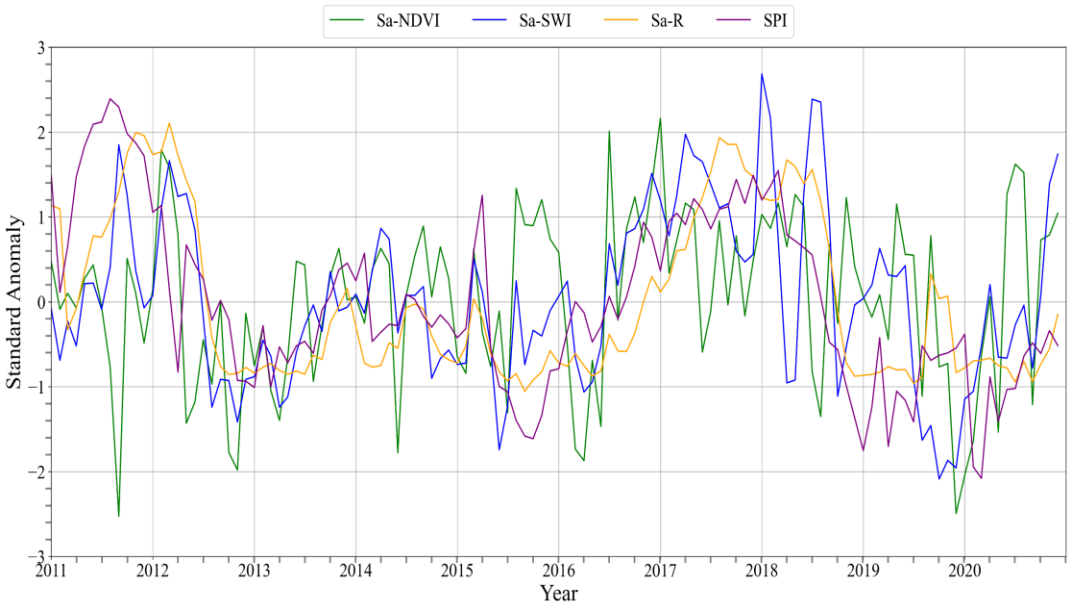

Fig. 7. SPI, Sa-NDVI, Sa-SWI, and Sa-R time series from 2011–2020.

Table 2.
Correlation coefficient between drought indices during before harvest, rice yield and reservoir storage in the Chi River basin.

	SPI	Sa-NDVI	Sa-SWI	Sa-R	ANDI
Rice yield (dry)	0.61	0.67	0.48	0.86	0.80
Reservoir (dry)	0.88	0.77	0.65	0.85	0.90

Table 3.
Correlation coefficient between drought indices during end of rainy, rainfall in the Chi River basin.

	SPI	Sa-NDVI	Sa-SWI	Sa-R	ANDI
Rainfall (wet)	0.96	0.28	0.72	0.89	0.95

The combining of Sa-R with spatial data indices. Combining Sa-R with spatial data indices (Sa-NDVI and Sa-SWI) will assist to overcome this challenge.

Afterward, we estimated the weights of indices that were used to generate ANDI via the EW method. The results of this approach are provided in (**Table 4-5**), which were calculated in February. The weights of SPI, Sa-NDVI, Sa-SWI, and Sa-R are 0.22, 0.10, 0.11, and 0.57, respectively. However, this weight is unique for each month. The ANDI has correlations with rice yield, reservoirs, and rainfall of 0.80, 0.90, and 0.95, respectively (**Table 2-3**). It has the highest correlation with reservoir, while the correlation with rice yield is larger than SPI, Sa-NDVI, and Sa-SWI, and the correlation with rainfall is greater than Sa-NDVI, Sa-SWI, and Sa-R. ANDI also outperformed Sa-R and SPI in terms of pixel-difference. Therefore, ANDI was selected to represent drought conditions because it is well related to the drought situation in the dry and wet seasons (**Fig. 8**).

Table 4.

Practical Example of Entropy Weight Calculation in February.

		February									
P_{ij}	Year	2011	2012	2013	2014	2015	2016	2017	2018	2019	2020
	SPI	0.11	0.15	0.09	0.13	0.08	0.08	0.15	0.17	0.04	0.01
	Sa-NDVI	0.09	0.18	0.08	0.07	0.06	0.06	0.08	0.13	0.10	0.14
	Sa-SWI	0.06	0.14	0.07	0.09	0.06	0.10	0.13	0.19	0.10	0.05
	Sa-R	0.20	0.27	0.03	0.03	0.05	0.03	0.13	0.21	0.02	0.03
$ln(P_{ij})$	SPI	-2.25	-1.87	-2.45	-2.06	-2.47	-2.48	-1.93	-1.80	-3.21	-5.04
	Sa-NDVI	-2.40	-1.71	-2.55	-2.67	-2.81	-2.88	-2.47	-2.01	-2.25	-1.95
	Sa-SWI	-2.74	-1.96	-2.60	-2.43	-2.77	-2.26	-2.06	-1.68	-2.28	-3.02
	Sa-R	-1.59	-1.32	-3.62	-3.46	-2.98	-3.58	-2.08	-1.54	-3.97	-3.38

Table 5.

Entropy Weight for SPI, Sa-NDVI, Sa-SWI and Sa-R for combining into ANDI.

Indices	e_j	div_j	W_j
SPI	0.94	0.06	0.22
Sa-NDVI	0.97	0.03	0.10
Sa-SWI	0.97	0.03	0.11
Sa-R	0.83	0.17	0.57

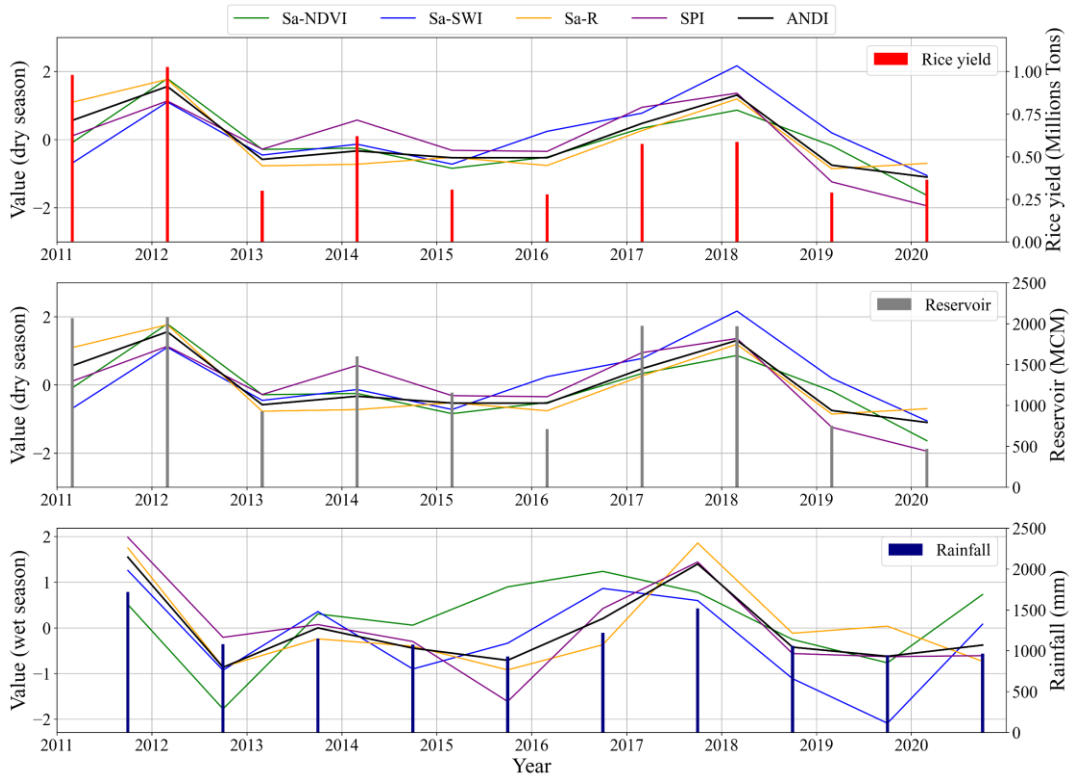

Fig. 8. Relationship between SPI, Sa-NDVI, Sa-SWI, and Sa-R and rice yield, reservoirs and rainfall.

4.2. Generation of ANDI drought hazard map

Remote sensing and GIS are used to produce the ANDI to investigate the spatial distribution of drought hazard areas in the basin with a 10 km^2 resolution. Most of the ANDI values in the 10 studied years (2011–2020) are between −1.5 and 1.5, but they are less than −0.5 when considering only the drought situation in the Chi River basin (2013, 2015, 2016, 2019, and 2020) (**Fig. 9**).

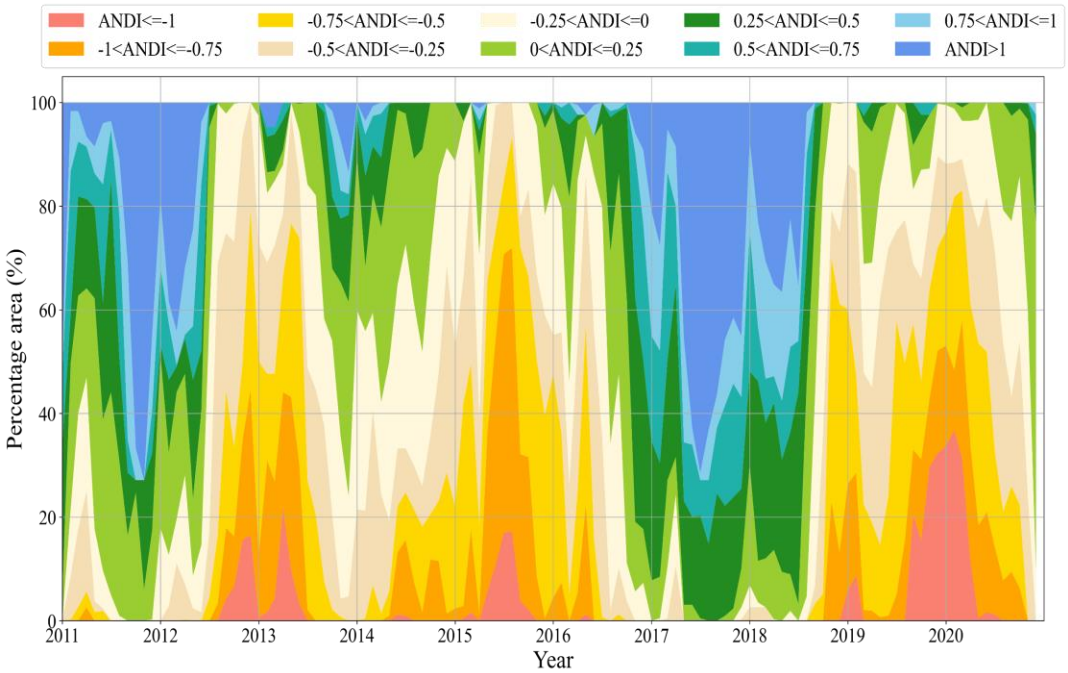

Fig. 9. Time series of monthly ANDI in the Chi River basin during 2011 – 2020.

According to data on rice yield, rainfall, and reservoir water quantities, drought occurred in 2013, 2015, 2016, 2019, and 2020. The initial ANDI, which was used to determine the occurrence of drought, was then examined.

In **Fig. 9**, the pink, orange, and yellow bars show the examined ANDI values of ANDI ≤−1, −1 < ANDI ≤ −0.75, and −0.75 < ANDI ≤ −0.5. Findings show that the ANDI of −0.25 is overvalued as a drought indicator because it sees areas in 2017 and 2018 that were not undergoing droughts. Moreover, the values of −0.75 and −1 are too small; they identify too little of the drought area in 2016. Thus, we set ANDI = −0.5 as the threshold for drought conditions in this study, and we established three drought levels for drought monitoring in the Chi River basin. **Fig. 9** shows the proportion of ANDI values dispersed in each range of ANDI values. Hence, we experimented with various random values to determine the appropriate value for the drought events (2013, 2015, 2016, 2019, and 2020). Then, we set the following ranges of drought levels: mild drought (−0.75 < ANDI ≤ −0.5), moderate drought (−1 < ANDI ≤ −0.75), and severe drought (ANDI ≤ −1).

The ANDI map was generated using the determined drought levels. There were three apparent droughts, namely, 2012 (wet) – 2013 (dry), 2014 (wet) –2016 (dry), and 2018 (wet) – 2020 (wet), all of which were followed by a wet season and then a dry season (**Fig. 10**). The drought event of 2019 – 2020 was the worst in 10 years, followed by those in 2012–2013 and 2014–2015; these severe droughts affected 37%, 22%, and 17%, respectively, of the basin.

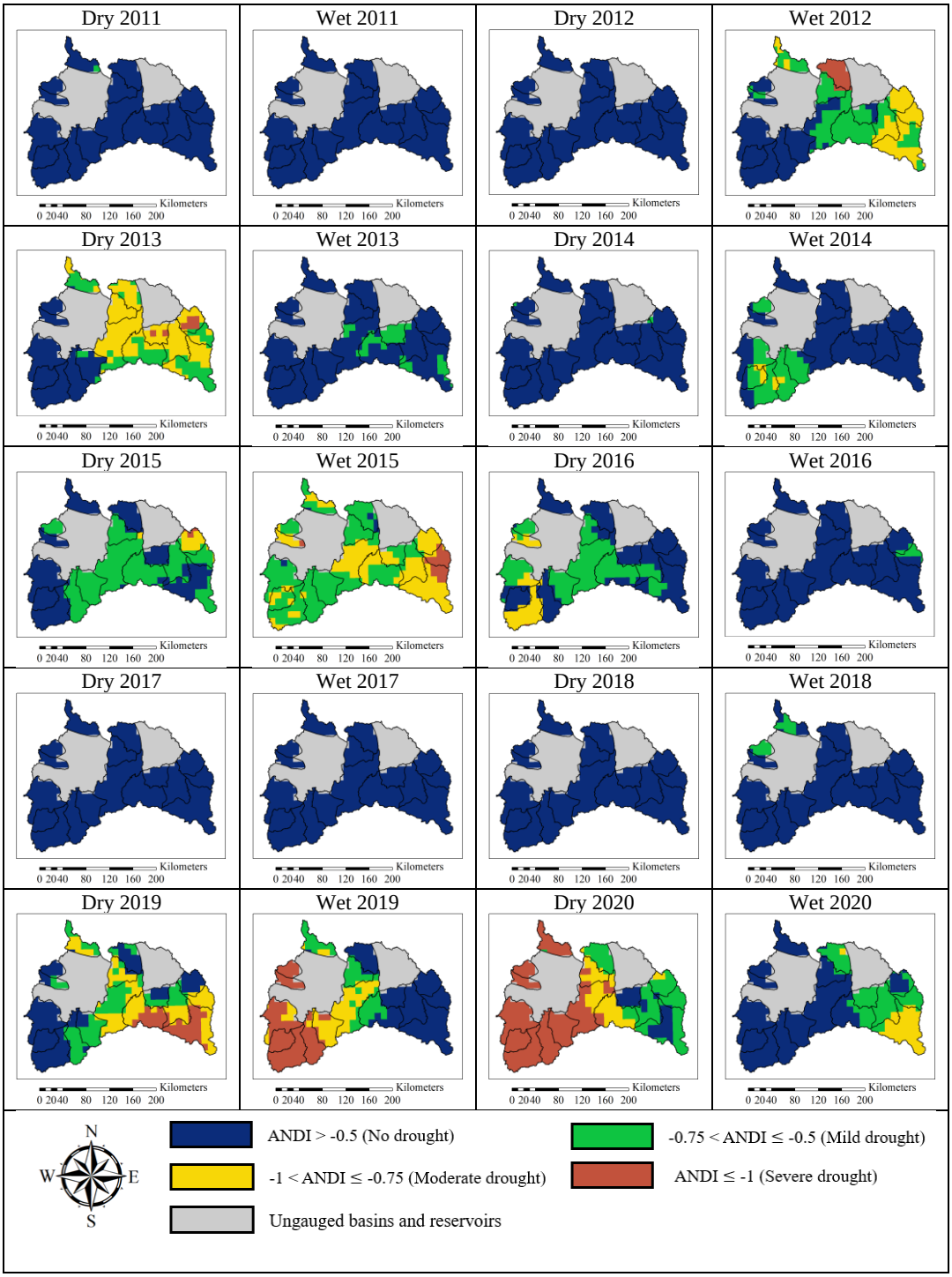

Fig.10. Drought hazard map in the Chi River basin based on the ANDI during 2011–2020.

4.3. Validation of ANDI map with reported drought events

Data on drought occurrences in the Chi River basin were collected from the georeferenced EM-DAT (https://public.emdat.be/data accessed on 1 March 2022) and the NHC (https://tiwrm.hii.or.th/v3/archive accessed on 1 March 2022). The EM-DAT contains three disaster reports of drought in the Chi River basin in 2011–2020. In 2012, the April–August drought incurred damages of $1.2 million. From January 2015 to May 2017 (2 years and 4 months), the long, intense drought incurred a total damage value of $3.3 billion. The last recorded drought occurred in July 2019 and lasted 6 months, but no damage was reported (**Table 6**). The NHC contains data about five drought events that occurred during 2011–2020 (2013, 2014, 2015, 2016, and 2020), which may have occurred during the dry season (November–April). According to a comparison between the ANDI map's drought assessment results and the drought situation reports from the CRED and NHC, the ANDI map's assessment is consistent with that of EM-DAT during 2015, 2016, and 2020 but not in 2017 and 2019. It is also consistent with drought data from the NHC for 2013, 2015, 2016, and 2020 but not for 2014 and 2019. A comparison of EM-DAT and NHC data shows corresponding drought events during dry seasons in 2015, 2016, and 2020. This is consistent with the drought analysis results from the ANDI map; inaccuracies are observed for 2019 (**Table 7**).

In Thailand, several research articles on drought monitoring have been published. In 2019, Zenkoji et al. analyzed drought in the upper Chao Phraya River basin using data on rainfall and dam inflows of large reservoirs (Bhumibol Dam and Sirikit Dam) during 1953–2015; their findings showed that droughts occurred in 2012–2015, especially in 2015, when the worst drought occurred (Zenkoji et al., 2019). Raksapatcharawong et al. (2020) studied droughts in 2012, 2014, 2015, 2018, and 2019 using information gathered from the Department of Agricultural Extension and concluded that northeast Thailand experienced the greatest impact. Jomsrekrayom et al. (2021) conducted a study on droughts in the northeast region of Thailand using VCI values from MODIS products; their results showed droughts during the wet seasons of 2011, 2012, 2013, 2017, 2018, and 2019, with those in 2013 and 2019 being severe ones. The drought assessment results from these previous studies show droughts in 2012, 2013, 2014, 2015, 2018, and 2019 in agreement with the ANDI drought assessment results.

Table 6.

Drought hazard events in Thailand from EM-DAT

Disaster No.	Disaster Type	Country	Start year	Start month	End year	End month	Total Damages (US$)
2012-9109-THA	Drought	Thailand	2012	4	2012	8	1,200,000
2015-9574-THA	Drought	Thailand	2015	1	2017	5	3,300,000,000
2019-9359-THA	Drought	Thailand	2019	7	2020	2	-

Table 7.

Comparison of drought hazard results of the ANDI with EM-DAT and NHC data.

Year	2011		2012		2013		2014		2015		2016		2017		2018		2019		2020	
Season	D	W	D	W	D	W	D	W	D	W	D	W	D	W	D	W	D	W	D	W
ANDI			✓		✓			✓	✓	✓	✓						✓	✓	✓	
EMDAT			✓						✓	✓	✓	✓	✓					✓	✓	
NHC			✓		✓	✓	✓	✓	✓	✓	✓							✓	✓	
Combined			✓						✓	✓	✓							✓	✓	

5. CONCLUSIONS

Drought analysis in the Chi River basin using the proposed ANDI, a composite index incorporating SPI, Sa-NDVI, Sa-SWI, and Sa-R, is conducted from a combination analysis of satellite data and station measurement data. The NDVI and SWI values are based on MODIS and ASCAT products, respectively, whereas SPI is based on precipitation and utilizes IDW to distribute into pixels. Runoff measurements are used to construct runoff maps. All four data points are connected to various drought scenarios. The SPI detects variations in precipitation, the NDVI distinguishes agricultural and non-agricultural places, the SWI shows soil moisture, and runoff indicates the quantity of water farmers may utilize at a given moment.

ANDI outperforms other indices in its association with the reservoir during the dry season, but it performs similarly to Sa-R and SPI in its link with rice yield during the rainy season. Furthermore, ANDI is more efficient than the Sa-R and SPI for estimating droughts in any season.

Drought occurs during the dry season and is driven mostly by water scarcity; during the wet season, it is influenced primarily by rainfall. The ANDI is analyzed and compared with drought event data from 2011 to 2020 to establish drought severity levels. During times of drought, most ANDI values are below −0.5. Therefore, the ANDI value of −0.5 is set as the threshold for entering a drought state. Then, the following drought levels are set: mild drought ($-0.75 < \text{ANDI} \leq -0.5$), moderate drought ($-1 < \text{ANDI} \leq -0.75$), and severe drought ($\text{ANDI} \leq -1$). Drought analysis using the ANDI and the defined levels shows that each drought occurred during the wet season and arrived during the dry season because of the low rainfall during the wet season. This results in insufficient water supply in dams during dry seasons. Additionally, findings indicate a total of 5 years of drought (2013, 2015, 2016, 2019, and 2020). For 2015, 2016, and 2020, the ANDI drought assessment results agree with EM-DAT and NHC drought reports. Therefore, the ANDI can assess drought effectively (close to actual events) and is a good tool for monitoring and assessing future droughts.

ACKNOWLEDGEMENTS

The authors appreciatively thank the Land Development Department for land use data, the Royal Irrigation Department for rainfall and runoff data, and the Hydro Informatics Institute (HII) for recording water events. Kantawong was supported by the M.ENG scholarship by the Kasetsart University (65/19/WE/M.ENG).

REFERENCES

Albergel, C., Rudiger, C., Pellarin, T., Calvet, J.C., Fritz, N., Froissard, F., Suquia, D., Petitpa A., Piguet, B., Martin, E. (2008) From near-surface to root-zone soil moisture using an exponential filter: an assessment of the method based on in-situ observations and model simulations. *Hydrology and Earth System Sciences*. 12(6), 1323-1337.

Amri, R., Zribi, M., Lili-Chabaane, Z., Duchemin, B., Gruhier, C., Chehbouni, A. (2011) Analysis of vegetation behavior in a North African semi-arid region, using SPOT-VEGETATION NDVI data. *Remote sensing*. 3(12), 2568-2590.

Amri, R., Zribi, M., Lili-Chabaane, Z., Wagner, W., Hasenauer, S. (2012) Analysis of C-band scatterometer moisture estimations derived over a semiarid region. *IEEE transactions on geoscience and remote sensing*. 50(7), 2630-2638.

Anderson, M.C., Zolin, C.A., Sentelhas, P.C., Hain, C.R., Semmens, K., Yilmaz, M.T., Gao, F., Otkin, J.A., Tetrault, R. (2016) The Evaporative Stress Index as an indicator of agricultural drought in Brazil: An assessment based on crop yield impacts. *Remote Sensing of Environment*. 174, 82-99.

Bauer-Marschallinger, B., Paulik, C., Hochstöger, S., Mistelbauer, T., Modanesi, S., Ciabatta, L., Massari, C., Brocca, L., Wagner, W. (2018) Soil moisture from fusion of scatterometer and SAR: Closing the scale gap with temporal filtering. *Remote Sensing*. 10(7), p. 1030.

Bharathkumar, L., Mohammed-Aslam, M.A. (2015) Crop pattern mapping of Tumkur Taluk using NDVI technique: a remote sensing and GIS approach. *Aquatic Procedia*. 4, 1397-1404.

Bijaber, N., El Hadani, D., Saidi, M., Svoboda, M.D., Wardlow, B.D., Hain, C.R., Poulsen, C.C., Yessef, M., Rochdi, A. (2018) Developing a remotely sensed drought monitoring indicator for Morocco. *Geosciences*. 8(2), 55.

Brocca, L., Melone, F., Moramarco, T., Wagner, W., Hasenauer, S. (2010) ASCAT soil wetness index validation through in situ and modeled soil moisture data in central Italy. *Remote Sensing of Environment*. 114(11), 2745-2755.

Chen, S., Zhong, W., Pan, S., Xie, Q., Kim, T. W. (2020). Comprehensive drought assessment using a modified composite drought index: A case study in Hubei Province, China. *Water*, 12(2), 462.

Cui, A., Li, J., Zhou, Q., Zhu, R., Liu, H., Wu, G., Li, Q. (2021) Use of a multiscalar GRACE-based standardized terrestrial water storage index for assessing global hydrological droughts. *Journal of Hydrology*. 603, p. 126871.

Dracup, J.A., Lee, K.S., Paulson Jr, E.G. (1980) On the definition of droughts. *Water resources research*. 16(2), 297-302.

Gillespie, T.W., Ostermann-Kelm, S., Dong, C., Willis, K.S., Okin, G.S., MacDonald, G.M. (2018) Monitoring changes of NDVI in protected areas of southern California. *Ecological Indicators*. 88, 485-494.

Jomsrekrayom, N., Meena, P., & Laosuwan, T. (2021) Spatiotemporal analysis of vegetation drought variability in the middle of the northeast region of Thailand using terra/modis satellite data. *Geographia Technica*. 16, 70-81.

Kallis, G. (2008) Droughts. Annual review of environment and resources. 33, 85-118.

Marcos-Garcia, P., Lopez-Nicolas, A., Pulido-Velazquez, M. (2017) Combined use of relative drought indices to analyze climate change impact on meteorological and hydrological droughts in a Mediterranean basin. *Journal of Hydrology*. 554, 292-305.

McKee, T.B., Doesken, N.J., Kleist, J. (1993) The relationship of drought frequency and duration to time scales. In Proceedings of the 8th Conference on Applied Climatology, *California*, pp. 179-183.

Nanzad, L., Zhang, J., Tuvdendorj, B., Nabil, M., Zhang, S., Bai, Y. (2019) NDVI anomaly for drought monitoring and its correlation with climate factors over Mongolia from 2000 to 2016. *Journal of arid environments*. 164, 69-77.

Palmer, W.C. 1965. Meteorological drought. US Department of Commerce, Weather Bureau.

Pandey, S., Bhandari, H., Ding, S., Prapertchob, P., Sharan, R., Naik, D., Taunk, S.K., Sastri, A. (2007) Coping with drought in rice farming in Asia: insights from a cross-country comparative study. *Agricultural Economics*. 37, 213-224.

Paulik, C., Dorigo, W., Wagner, W., Kidd, R. (2014) Validation of the ASCAT Soil Water Index using in situ data from the International Soil Moisture Network. *International journal of applied earth observation and geoinformation*. 30, 1-8.

Prabnakorn, S., Maskey, S., Suryadi, F. X., de Fraiture, C. (2018) Rice yield in response to climate trends and drought index in the Mun River Basin, Thailand. *Science of the Total Environment*. 621, 108-119.

Raksapatcharawong, M., Veerakachen, W., Homma, K., Maki, M., Oki, K. (2020) Satellite-based drought impact assessment on rice yield in Thailand with SIMRIW− RS. *Remote Sensing*. 12(13), p. 2099.

Rouse Jr, J.W., Haas, R.H., Deering, D.W., Schell, J.A., Harlan, J.C. (1974) Monitoring the vernal advancement and retrogradation (green wave effect) of natural vegetation (No. E75-10354).

Shannon, C. E. (1948). A mathematical theory of communication. *The Bell system technical journal*, 27(3), 379-423.

Son, N.T., Chen, C.F., Chen, C.R., Chang, L.Y., Minh, V.Q. (2012) Monitoring agricultural drought in the Lower Mekong Basin using MODIS NDVI and land surface temperature data. *International Journal of Applied Earth Observation and Geoinformation*. 18, 417-427.

Teweldebirhan Tsige, D., Uddameri, V., Forghanparast, F., Hernandez, E.A., Ekwaro-Osire, S. (2019) Comparison of meteorological-and agriculture-related drought indicators across Ethiopia. *Water*. 11(11), p. 2218.

Tucker, C.J. (1979) Red and photographic infrared linear combinations for monitoring vegetation. *Remote sensing of Environment*. 8(2), 127-150.

Vicente-Serrano, S.M., Beguería, S., López-Moreno, J.I. (2010) A multiscalar drought index sensitive to global warming: the standardized precipitation evapotranspiration index. *Journal of climate*. 23(7), 1696-1718.

Waseem, M., Ajmal, M., Kim, T. W. (2015). Development of a new composite drought index for multivariate drought assessment. *Journal of Hydrology*, 527, 30-37.

Wichitarapongsakun, P., Sarin, C., Klomjek, P., Chuenchooklin, S. (2016) Rainfall prediction and meteorological drought analysis in the Sakae Krang River basin of Thailand. *Agriculture and Natural Resources*. 50(6), 490-498.

Wilhite, D.A., Svoboda, M.D., Hayes, M.J. (2007) Understanding the complex impacts of drought: A key to enhancing drought mitigation and preparedness. *Water resources management*. 21(5), 763-774.

Zarch, M. A. A., Sivakumar, B., Sharma, A. (2015). Droughts in a warming climate: A global assessment of Standardized precipitation index (SPI) and Reconnaissance drought index (RDI). *Journal of hydrology*, 526, 183-195.

Zenkoji, S., Tebakari, T., Dotani, K. (2019) Rainfall and reservoirs situation under the worst drought recorded in the Upper Chao Phraya River Basin, Thailand. *Journal of Japan Society of Civil Engineers, Ser. G (Environmental Research)*. 75(5), 115-124.

Zribi, M., Nativel, S., Le Page, M. (2021) Analysis of agronomic drought in a highly anthropogenic context based on satellite monitoring of vegetation and soil moisture. *Remote Sensing*. 13(14), p. 2698.

Zribi, M., Paris Anguela, T., Duchemin, B., Lili, Z., Wagner, W., Hasenauer, S., Chehbouni, A. (2010) Relationship between soil moisture and vegetation in the Kairouan plain region of Tunisia using low spatial resolution satellite data. *Water Resources Research*. 46(6), 823-835.